BULLETIN OF THE POLISH ACADEMY OF SCIENCES
TECHNICAL SCIENCES, Vol. 67, No. 3, 2019
DOI: 10.24425/bpasts.2019.129646

Digital image watermarking using fast parametric transforms

P. LIPINSKI and D. PUCHALA

Lodz University of Technology, 215 Wolczanska St., 90-924 Lodz, Poland

Abstract. This paper proposes a novel method for digital image watermarking, in which watermarks are embedded in the domain of fast parametric transforms based on known spread spectrum approaches. Fast parametric transforms have the ability to adapt the forms of base vectors, which enables automatic selection of the domain of watermarking in relation to the pair: a marked image – a watermarking attack. The process of adapting the forms of fast parametric transforms is carried out with aid of the classical genetic algorithm with the fitting function based on the known measure of separability of watermarks. The effectiveness of the proposed method has been verified experimentally on the basis of the images of two classes, i.e. natural images and technical diagrams. The results taking into account both the efficiency of watermark embedding and the generated distortions in the marked images are summarized in tables and accompanied by an appropriate commentary.

Key words: watermarking of digital images, fast parametric transforms.

1. Introduction

The greatest advantages of the present times include the ease of exchange and dissemination of information. A multimedia message has become the most popular form of transmission, in which information is transmitted as sound, image, or sound and image together. The availability of inexpensive data-archiving devices with large capacities, as well as the growing popularity of free data storage in the cloud, facilitate the unrestricted copying and redistribution of digital data without any effect on their quality. However, it is common knowledge in the information society, which we are part of, that information has grown to be a new commodity, on equal footing with material goods. Therefore, the universality of digital data, combined with their often high price, impose significant demands on modern multimedia technologies in the area of developing specialized intellectual protection mechanisms. The answer to this demand are the digital watermarking systems.

Digital watermarks are a new form of embedding information in digital images. The basic idea of digital image marking is to create metadata containing information about the protected image (i.e. information about the author, publishing institution, image content, etc.), then to convert the metadata to a form that allows easy embedment of the watermark (i.e. into a string of bits), and finally, to embed the metadata in the image itself. Once embedded, a watermark should be resistant to distortions resulting from the use of typical operations performed on images, such as: brightness or contrast adjustment, histogram equalization, noise reduction, etc. It should also be resistant to distortions caused by a deliberate attack aimed at complete removal or significant deformation of the embedded watermark (see [1]).

The basic applications of digital watermarking systems include: (a) copyright protection, where the watermark stores information identifying the copyright owner, (b) copy protection, where the watermark in combination with the legal installation requirements for mechanisms detecting watermarks in multimedia players (e.g. for DVD and Blu-Ray standards) allows to verify the legality of data copies, (c) fingerprint, where the watermark identifies the final recipient and on this basis allows to track down persons who distribute multimedia content, e.g. film distributors, without authorization, (d) content authentication, where the watermark can be used to verify the integrity of the content, and (e) monitoring the distribution of multimedia content, where the watermark allows to automatically trace the possible paths of data spread (see [1, 2]).

The most popular methods of digital images watermarking include those using discrete cosine transform (DCT) (see [3, 4]). In these methods, the watermark is embedded in the domain of DCT in the process of adding its subsequent elements to the selected transformation coefficients. In turn, the selection of the transformation, i.e. the domain of embedded watermarks, is dictated by the good properties of a DCT in the sense of condensation of a large amount of energy in a relatively small number of spectral coefficients. The high-amplitude coefficients, being the ones that carry a large amount of image information, are of particular interest from the point of view of watermarking (see [1,3]). However, DCT have good energy condensation properties, understood statistically, for the class of signals modeled as Markov first-order processes with high values of the autocorrelation coefficient (see [5]). This means that there is still a possibility to select in the process of optimization a transform with better properties than a DCT to go with a specific signal, in this case an image (see [6]). In the class of linear transforms, it is the fast parametric transforms (FPTs) that have adaptation prop-

*e-mail: piotr.lipinski@p.lodz.pl

Manuscript submitted 2018-07-14, revised 2018-08-24, initially accepted for publication 2018-10-08, published in June 2019.

erties (see [7]). FPTs constitute a generalization of known fast linear transforms, i.e. the Walsh-Hadamard, Hartley, Fourier, or cosine and sine transforms of various types, etc., into the class of adaptable transformations. Adaptation itself is possible thanks to the parameterization of fast computational structures for linear transforms. Thus, with appropriately selected parameter values, FPTs become well known fast linear transformations. Otherwise, they can be adapted to the statistical characteristics of the input data or to the specific requirements of the tasks being performed. This property makes FPTs a powerful tool for digital signal processing.

Having in mind the diversity and importance of potential application areas, it is clear that the development of novel methods of watermarking of images, that offer high efficiency and resistance corresponding to the current needs, is a very important and timely task. Bearing in mind the high potential of FPTs, this paper puts forward a novel method for watermarking of images, in which the watermarking process is carried out in the domain of fast parametric linear transformations. The form of a fast parametric transform is then selected automatically in the adaptation process, in line with the criterion of increasing the efficiency of watermarking and its resistance to possible attacks. The effectiveness of the proposed method was verified experimentally using test images.

2. Image watermarking systems

Image watermarking systems are classified against the following criteria: (a) in relation to the underlying concept used, e.g. substitution of image representation elements, spread spectrum, or quantization index modulation (QIM) [8], (b) in relation to the method of embedding a watermark, where the additive or quantizing approaches can be distinguished, (c) in relation to additional information passed to the watermark detector, i.e. uninformed and informed strategies, and (d) in relation to the domain of watermarking, where the spatial domain, the domain of discrete Fourier transform (DFT), the discrete cosine transform (DCT), and the discrete wavelet transform (DWT) can be specified (see [1,2]). Further on in this section, a brief review of existing methods was carried out, ranking them against the first of the criteria outlined above.

Image watermarking by substitution is an example of the elementary concept, in which the watermarking process consists in a simple replacement of parts of the binary representations of selected elements of the image being marked for binary expansions of the elements of the watermark (see [9–11]).

In the case of spread spectrum concept, the watermark is embedded in the domain of a linear transformation, most often a DCT or a DWT, in the process of scattering the energy of its individual elements in groups of spectral coefficients of transforms that lie within the scope of visually significant frequency bands. Clearly, the disturbance introduced must be small enough not to cause visible changes in the image itself. This action guarantees a high resistance of the watermark to possible attacks while maintaining a good quality of the marked image. Some of the methods that use this concept include the following algorithms: Cox et al. [3], Barni et al. [4], Lee et al. [12], Wei et al. [13] in the case of DCT, or Dugad et al. [14], Tsekeridou and Pitas [15], and Barni et al. [16] for DWT (see [1]). The algorithms [3–16] are at the same time an example of additive approaches, i.e. those in which the watermarking process is carried out by adding the values of its individual elements to the values of transform coefficients. Hybrid approaches are also known (see e.g. [23, 24]), in which the domains of both DCT and DWT are used simultaneously. This combination allows to take advantage of the characteristic properties of the two transformations to increase the resistance of watermarking, i.e. the properties of high energy concentration in a small number of DCT spectral coefficients, as well as a good spatial location and the possibility of multiresolution analysis in the case of DWT.

QIM approaches refer to a class of non-linear methods based on scalar or vector quantization. In the QIM approach, quantization operations are used to increase the distance between the image and the watermark being embedded. In turn, the watermarking process itself can be implemented both in the spatial domain and in the domain of linear discrete transforms (DFT, DCT, or DWT). As examples, the known algorithms of Xie and Arce [25], Chu and Wilz [26], or Li and Xue [27] can be indicated.

3. Evaluation of digital image watermarking systems

The most important measures describing the properties of digital images watermarking systems include: the watermarks embedment efficiency, the amount of distortion introduced into the marked image, and the information capacity.

Embedment efficiency. It is a measure of the probability that a digital watermark will be detected after it is embedded [28]. In practical applications, two measures of effectiveness are most often used. These are: the FMR (false match rate) – the probability of detecting a watermark in the case when it has not been embedded, and the FNMR (false non-match rate) – the probability of not detecting a watermark despite its embedding.

In this study, we use a different measure of effectiveness, originally proposed in monograph [1]. This measure is the separability s, defined here in accordance with the following relation as:

$$s = \min_{l=0,1,\ldots,K-1} \left\{ \min_{\substack{k=0,1,\ldots,K-1 \\ k\neq l}} \left\{ |\rho_{w_l w_l^*} - \rho_{w_l w_k^*}|_\star \right\} \right\}, \quad (1)$$

where $|\cdot|_\star$ is a truncated absolute value equal to zero for negative arguments, whereas $\rho_{w_l w_l^*}$ for $l \in \{0,1,\ldots,K-1\}$ is the correlation coefficient calculated between a fixed watermark w_l and its extracted form w_l^*, while $\rho_{w_l w_k^*}$ for $k = 0,1,\ldots,K-1$ denotes the correlation coefficients calculated between the specific mark w_l and the extracted forms of other randomly selected watermarks w_k. In Fig. 1, a graphical interpretation of the separability measure for one fixed mark w_l (for $l = 24$) and a set $K = 100$ watermarks is shown. Therefore, the value of this mea-

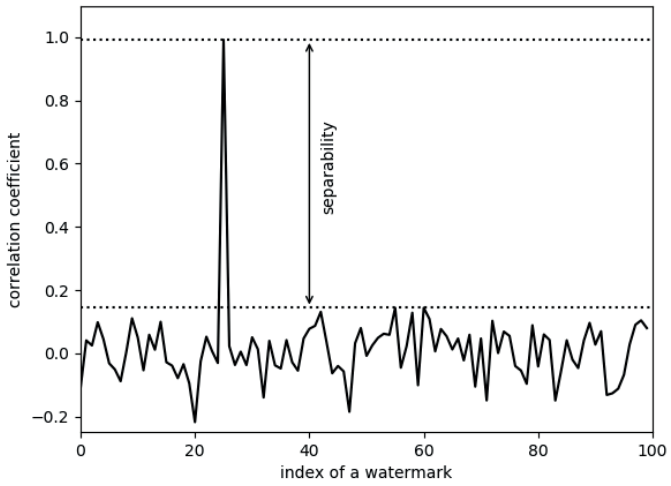

Fig. 1. Interpretation of the watermark separability measure determined for one selected watermark taken from the set of $K = 100$ watermarks

sure can be interpreted as a safe distance allowing for separation of a given watermark from other watermarks in the sense of correlation values at the stage of extraction. This measure becomes a single indicator of the effectiveness of the watermarking system, which in turn is convenient to use in the process of adaptive selection of the domain of embedding. In addition, the increase in separability clearly improves watermarking efficiency understood in the sense of FMR and FNMR measures. The value of the correlation coefficient is then determined according to the formula:

$$\rho_{w_l w_k^*} = \left(\frac{\frac{1}{M}\sum_{m=0}^{M-1}(w_l(m)-\mu_{w_l})(w_k^*(m)-\mu_{w_k^*})}{\sigma_{w_l}\sigma_{w_k^*}} \right), \qquad (2)$$

where μ_{w_l} and $\mu_{w_k^*}$ are the expected values of the elements of the watermarks w_l and w_k^* which we define as:

$$\mu_{w_l} = \frac{1}{M}\sum_{m=0}^{M-1} w_l(m), \qquad \mu_{w_k^*} = \frac{1}{M}\sum_{m=0}^{M-1} w_k^*(m),$$

while σ_{w_l} and $\sigma_{w_k^*}$ are standard deviations of watermark elements calculated according to the formulas:

$$\sigma_{w_l} = \sqrt{\frac{1}{M}\sum_{m=0}^{M-1}\left(w_l(m)-\mu_{w_l}\right)^2},$$
$$\sigma_{w_k^*} = \sqrt{\frac{1}{M}\sum_{m=0}^{M-1}\left(w_k^*(m)-\mu_{w_k^*}\right)^2},$$

where $l,k \in \{0,1,\ldots,K-1\}$.

Image distortion. Embedding a watermark in a digital image, whether in the spatial domain or in the domain of linear transformations, involves introducing certain distortion to the image. In the case of additive techniques, i.e. those where the watermark is added to the elements of image representation (see Section 5), this distortion will be equal to the energy of the embedded watermark. To evaluate the level of distortion or image quality, different measures are used, with the most popular being the peak signal-to-noise ratio (PSNR) in the case of measures with mathematical origin, and the structural similarity index measure (SSIM) for measures relating to the model of human image perception (see [1]). Both measures were used in this study, and they can be defined according to the equations (3) and (4).

Let X_0 be a grayscale image (only the luminance component) with a resolution of N_1 on N_2 pixels. Then, by $\{X_0(i,j) : i = 0,1,\ldots,N_1-1, j = 0,1,\ldots,N_2-1\}$ we will describe a set of pixels of the image X_0. An image with an embedded watermark w will be designated, respectively, as X_w. Then, we can define the PSNR image quality measure as:

$$\mathrm{PSNR} = 10\log_{10}\left(\frac{X_{\max}^2}{\mathrm{MSE}}\right), \qquad (3)$$

where $X_{\max}$ is the maximum possible pixel value (assumed *a priori* to be $X_{\max} = 255$), and MSE is a mean square image distortion measure calculated using the formula:

$$\mathrm{MSE} = \frac{1}{N_1 N_2}\left(\sum_{i=0}^{N_1-1}\sum_{j=0}^{N_2-1}(X_0(i,j)-X_w(i,j))^2\right).$$

The above mentioned measures PSNR and MSE allow to measure the level of global distortion in the image, which means that they do not account for local image characteristics. The measure that takes into account these characteristics is SSIM. Then we have:

$$\mathrm{SSIM} = \frac{(2\mu_{X_0}\mu_{X_w}+\beta_1)(2\rho_{X_0X_w}+\beta_2)}{(\mu_{X_0}^2+\mu_{X_w}^2+\beta_1)(\sigma_{X_0}^2+\sigma_{X_w}^2+\beta_2)}, \qquad (4)$$

where μ_{X_0} and μ_{X_w} are the mean values of the pixels from images X_0 and X_w, whereas σ_{X_0} and σ_{X_w} are the standard deviations of pixel values for both images, β_1 and β_2 are constants, stabilizing the result when the denominator approaches zero (we assumed that $\beta_1 = 0$ and $\beta_2 = 0$), while:

$$\rho_{X_0X_w} = \frac{1}{N_1 N_2}\left(\sum_{i=0}^{N_1-1}\sum_{j=0}^{N_2-1}(X_0(i,j)-\mu_{X_0})(X_w(i,j)-\mu_{X_w})\right)$$

is the coefficient of covariance of images X_0 and X_w.

Information capacity. It is defined as the number of watermark bits that can be embedded in an image or in its representation in the domain of a linear transformation. Although information capacity is a very important issue, for the sake of the profile of this research study, we consider it as of secondary importance, using only the parameter M, which determines the length of the watermark. Clearly, the amount of information stored will depend directly on the length of the watermark. During experimental investigations, the value of parameter M is arbitrarily set in a way that allows obtaining a high efficiency of embedding with respect to the measure s, with acceptable levels of distortion.

It should be noted that the measures described above can be mutually opposed. For example: increasing the resistance of a watermark will require to increase its length M, or to increase the strength of embedding by adjusting the coefficient η, which in turn is associated with an increase in the introduced distortion to the image. Thus, the adaptation process must be properly balanced so as not to improve one of the indicators at the cost of an unacceptable decrease in the others.

4. Fast parametric transforms

Fast parametric transforms (FPTs) are linear transformations with fast computational structures, i.e. they can be characterized by computational complexity of the order $\mathcal{O}(N \log_2 N)$, where N is the size of the transform. In addition, FPTs thanks to the parameterization have the ability to adapt to both the statistical characteristics of the processed data, as well as to the specific requirements of the performed task [7]. The property of adaptation is therefore a key advantage of parametric transforms over known transformations with fixed base vectors, such as Haar, Walsh-Hadamard, Hartley, or cosine and sine transforms of various types (see [5, 29]). Fast computational structures of FPTs can be selected arbitrarily, i.e. they can result directly from design rules developed to obtain transforms with specific properties, e.g. involutory transforms [30], or they can duplicate structures of known fast discrete transforms, as in Slant transform [31] or the Walsh-Hadamard transform [32]. The adaptation process, i.e. the process of parameter values selection, can be implemented using any techniques that should be, however, properly selected to meet the needs of the task being at hand. If the objective function can be described as a differentiable function, gradient techniques can be used (see [7]). Otherwise, it will be necessary to use evolutionary approaches, e.g. genetic algorithms [33, 34, 36] or swarm algorithms [35, 36].

The FPT structure used in this paper. In this study, a two-stage structure of a fast cosine transform of type II (DCT-II) was used. The choice of a structure that can realize the DCT-II is crucial since the cosine transformation has good properties from the point of view of watermarking of digital images, as demonstrated in many studies (see [3, 4, 9–13, 16]). The used in this paper structure of FPT for the case of $N = 8$ points is depicted in Fig. 2. At this point, it should be stressed that the first stage of transformation, i.e. the stage realizing orthogonal linear combinations of input sequence elements using elementary base operations calculating the sum/difference of elements at the input, where these operations were graphically marked as "$\circ$", was not a subject to parameterization. The parameterization only concerned the second stage consisting of planar rotation operations O_{ij} for $i = 0, 1, \ldots, \log_2 N - 1$ and $j = 0, 1, \ldots, N/2 - 1$, which are designated as "$\bullet$". The angles of rotations α_{ij} in the number of $\mathscr{L}_{PAR} = (N/2) \log_2 N$ are then a set of parameters describing the form of FPT, the values of which are subject to selection in the adaptation process. The decision about the partial parameterization of the structure was made due to the high dimensionality of the search space, which is e.g. $\mathbb{R}^{1024}$ for $N = 256$ points.

It should be noted that fast parametric transforms with such computational structures enable their effective implementations in parallel or massively-parallel approaches using graphics processing units (GPU) (c.f. [17, 18]). The GPU accelerated algorithms constitute dynamically developing branch of computational techniques used extensively in many practical engineering problems (see e.g. [19–22]).

Inverse fast parametric transform (IFPT). The FPTs considered in this work are orthogonal transformations. If U were to designate a forward transformation matrix, then the inverse transform would take the form of U^T. In the case of graph structures (see Fig. 2), the transposition operation means reversing the order of individual steps for $i = 0, 1, \ldots, \log_2 N - 1$ composed of base operations O_{ij}, and within the mentioned steps it is required to invert the individual base operations, i.e. O_{ij}^T for $j = 0, 1, \ldots, N/2 - 1$. It should be noted that in the case of the structure from Fig. 2, additional scaling of the IFPT results by the factor $2/N$ (or each of FPT and IFPT transformations by $\sqrt{2/N}$) is required. This is due to the lack of normalization of base operations marked symbolically as "$\circ$".

Adaptation of FPT. Taking into account the functional requirements of the considered in this paper implementation variants of the proposed method, the classical genetic algorithm was chosen

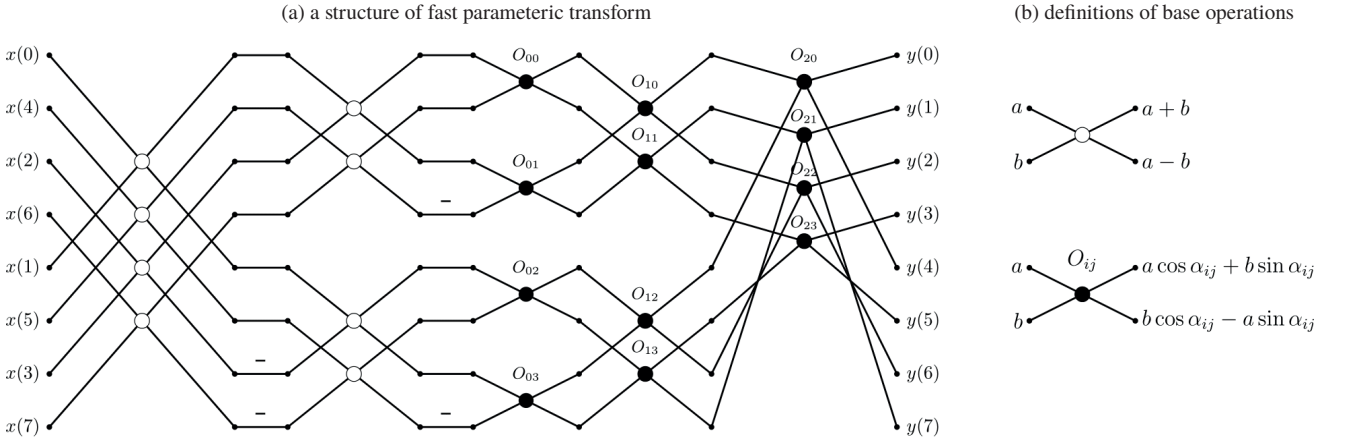

Fig. 2. Structure of a fast parametric transform for the case of $N = 8$ points (a), definitions of base operations (b)

for the purpose of adapting the values of FPT parameters (see [33, 34]). It should be noted that the form of FPT (i.e. the set of parameters) is selected in relation to the maximization of the separability s measure of watermarking efficiency, which was described in Section 2. The watermarking process itself is carried out in the domain of FPT according to the scheme shown in Fig. 6 or Fig. 7, which in turn depends on the considered variant of implementation. The quality of the watermark extraction expressed by the correlation measure (see formula (2)), and thus the separability value s, is primarily influenced by possible attacks. Each attack introduces distortions to the image, which can significantly hinder or even prevent the correct extraction of the watermark. Thus, taking into account both the specifics of watermarking schemes considered, as well as the characteristics of possible attacks (i.e. low-pass filtration, contrast change, sharpening filtering, histogram equalization, etc.), it would be extremely difficult to describe the entire path that determines the value of the separability measure in the form of a mathematical function. Hence the choice of evolutionary approaches, in case of which only the evaluation of the specific set of parameters by calculating the separability measure s is required, which in practice only means the need to define the *fitness function*, as opposed to gradient approaches, where a differentiable mathematical function describing the whole scheme of watermark embedding and extraction is required.

To determine the adaptation function, the method of coding the values of FPT parameters in the form of gene sequences that further compose chromosomes should be determined first. In this paper, the method of coding the values of angles of rotation α_{ij} for individual base operations in the form of binary extensions of L-bit integer numbers has been adopted. In this case, the parameter value expressed in radians will be determined based on the following formula:

$$\alpha_{ij} = 2\pi b_{ij}/2^L \tag{5}$$

for $i = 0, 1, \ldots, \log_2 N - 1$ and $j = 0, 1, \ldots, N/2 - 1$, with numbers $b_{ij} \in \{0, 1, \ldots, 2^L - 1\}$ being the L-bit integers describing

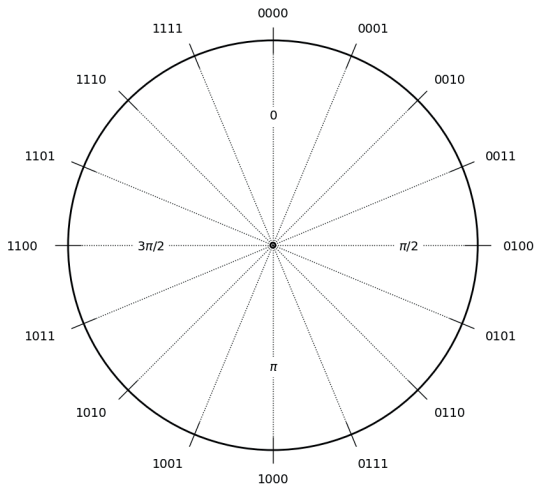

Fig. 3. The way of mapping the parameter value (in a binary expansion) to the rotation angle, i.e. mapping of b_{ij} to the value α_{ij} for $L = 4$ bits

the quantized values of the angles of rotation α_{ij}. This corresponds to the quantization of the entire range $[0, 2\pi)$ of the variability of the parameter's value to the number 2^L of discrete values (compare Fig. 3 for the case $L = 4$). Thus, the *genotype*, expressed in the form of a single chromosome will take the form of a series of binary numbers with a length of $\mathscr{L}_{PAR} \cdot L$ elements, where the subsequent L-bit sequences are binary expansions of numbers b_{ij} (see Fig. 4a for the case of $L = 8$). In addition, in the used implementation of the genetic algorithm, elementary single-point crossover and mutation operations were used (compare Fig. 4b and c), and the step of selecting the best-matched individuals was based on the roulette wheel algorithm (see [33, 34]).

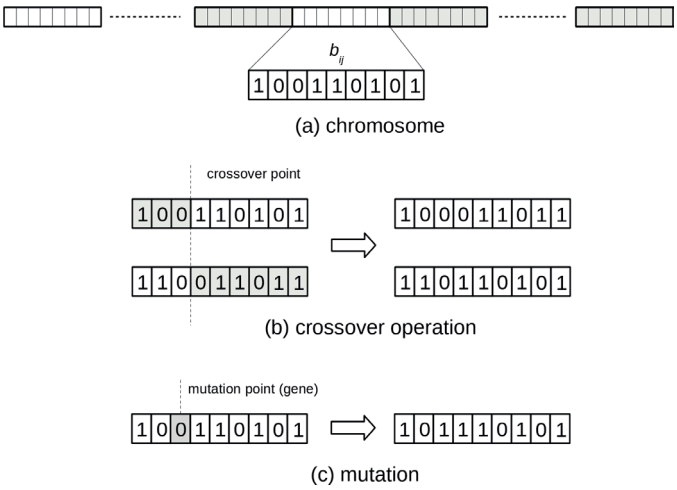

Fig. 4. Form of the chromosome (a), single-point crossover (b) and mutation (c) operations

5. The proposed method of image watermarking

An essential novelty introduced by the method proposed in this paper is the use of fast parametric linear transforms to determine the domain of watermarking. The forms of these transformations are selected automatically in the process of adaptation that takes into account the classes of watermarks, the selected types of attacks, and the images being marked. The decision to make a research study aimed at verifying the effectiveness of FPTs in the tasks of watermarking of images was motivated by the results contained in [1, 37, 38]. The results obtained there indicated a significant improvement of the resistance of watermarks embedded in the domain of DWT at a time when the coefficients of filters for wavelet transforms were selected automatically in the adaptation process. The genetic algorithm was also used in [13] to determine the location of the DCT coefficients in which the watermark should be embedded.

In this paper, two implementation variants of the proposed method were considered, i.e. the first variant, which is the implementation of the Cox et al. algorithm [3], as well as the second variant, based on the Barni et al. approach [4]. The block diagram for the first variant is shown in Fig. 6. According to the scheme, an input image subjected to watermarking is trans-

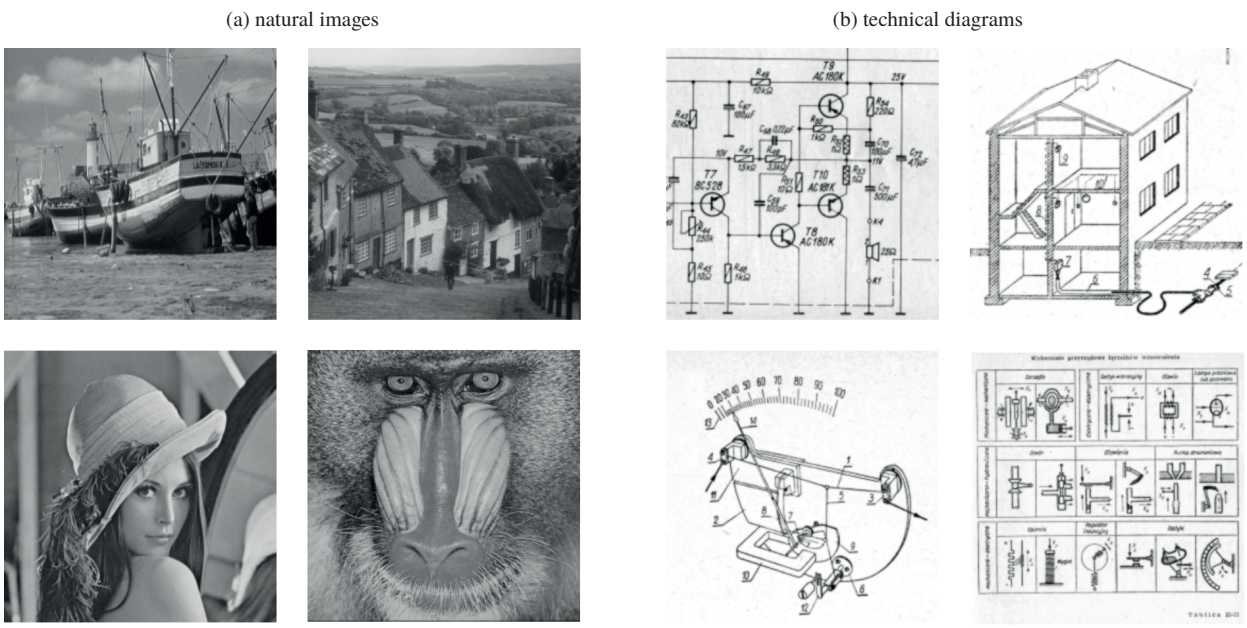

Fig. 5. Test images used during experimental research: a) natural images, b) technical diagrams

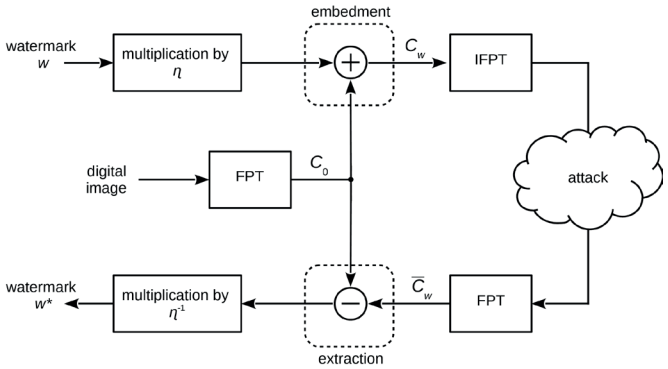

Fig. 6. Block diagram of the first variant of the proposed method

formed into a FPT domain, the form of which was previously selected in the adaptation process. As a result, the image representation C_0 is obtained in the domain of FPT. Then, to the first M coefficients, largest in terms of amplitude, the following elements of the watermark are added, which were previously multiplied by the coefficient η defining the strength of the embedding process. The parameter M also determines the length of the watermark. The result of this operation is a marked C_w image representation in the FPT domain. This operation can be symbolically described as:

$$C_w(i) = C_0(i) + \eta w(i), \tag{6}$$

for $i = 0, 1, \ldots, M-1$ where w is a watermark with the length of M elements. The next step is an inverse fast parameteric transform (IFPT), which makes it possible to return to the spatial domain. Further, the watermarked image may be made public, e.g. by posting it on the Internet, where it may be subject to intentional or accidental attacks such as lossy compression, noise reduction filtering, change in brightness and contrast, histogram equalization, etc. (c.f. [1, 39]). The watermark extraction is carried out in the domain of FPT. The representation of a marked image in the FPT domain with possible distortions resulting from potential attacks is referred to here as $\overline{C}_w$. The watermark is extracted based on the following relation:

$$w^*(i) = \left(\overline{C}_w(i) - C_0(i)\right)/\eta \tag{7}$$

for $i = 0, 1, \ldots, M-1$. The last step in the diagram from Fig. 6 is a division by the η factor. It should be noted that in the process of watermark extraction, knowledge of the original image to be marked (or rather its representation in the domain of FPT) is required.

The second of the considered implementation variants was based on the image watermarking algorithm presented in [4]. The method of operation of this algorithm is depicted in the block diagram from Fig. 7. The differences between both vari-

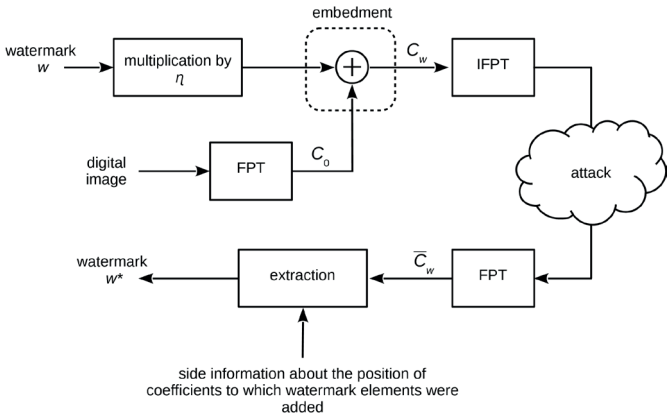

Fig. 7. Block diagram of the second variant of the proposed method

ants can be observed at the stage of watermark extraction. In the second variant, no knowledge of the input image is required. The necessary additional information is a knowledge of the position of coefficients in the domain of transformation, to which the subsequent elements of a watermark were added according to the formula (6). Then, the extracted watermark w^* will then be a set of M transformation coefficients taken with the assumed order. In this work, the Zig-Zag sequence has been adopted because it is constant and independent from the image contents. This way of selection of coefficients in the transformation domain is well known from the JPEG standard (see [5]) because it sufficiently well approximates the ordering of DCT coefficients relative to a non-increasing energy.

According to the typology of watermarking methods presented at the beginning of this section, both variants should be classified as Spread Spectrum methods. Of course, in the case of a parameteric transform, the spectral interpretation of its individual base vectors is not constant because it depends strictly on the values of the transform parameters, i.e. on the form of the transformation itself. In both variants, watermarks are embedded in an additive manner. However, in relation to the watermark extraction stage, the first variant should be classified as an informative method, because the knowledge of the input image is required, whereas the second one is an example of an uninformed (blind) approach. In addition, considering the adaptive selection of the domain of watermarking, both variants can be classified into a group of methods involving informed embedding (see [2]).

The essence of the proposed method is the use of fast parametric transforms for the purpose of embedding watermarks in images according to the Spread Spectrum scheme. The FPT domain, then, becomes the domain of watermarking. The form of FPT is selected automatically in the adaptation process according to the criterion of maximizing the effectiveness of watermarking and resistance to possible attacks. The adaptation process is carried out taking into account the specific image, attack, and a class of watermarks. In addition, two implementation variants of the proposed method were considered based on known watermarking algorithms operating in the domain of linear transforms, as proposed in [3] and [4], respectively (see also Figures 6 and 7). This requires, in particular, the formulation of procedures for embedding and extraction of watermarks, as well as the procedure for adaptation of FPT.

Let X_0 be an input grayscale image with a resolution of N on N pixels (i.e. $N_1 = N_2 = N$), whereas N is an integer power of two, i.e. $N = 2^n$, where n is a positive integer number. By w_0 we denote further on the M-element watermark embedded in the domain of FPT of a given form (symbolically described by matrix U), whereas the factor η determines the embedding force. The procedure for embedding the watermark is formulated below.

Procedure I (Watermark embedding).

1. Transform an input image X_0 into the domain of a two-dimensional FPT using the row-column approach (linear transformation separability is assumed here). This step can be performed based on the fast FPT algorithm, first by transforming individual rows (columns) of the image, followed by columns (rows). If U is an FPT matrix, then the obtained representation in the matrix notation will take the following form: $C_0 = UX_0U^T$.
2. Embed the watermark w_0 in the C_0 image representation according to the formula (6) depending on the method variant: in the number of M largest (in terms of absolute values of amplitude) coefficients of C_0 (for the first variant), or in the number of M first coefficients of C_0 taken in accordance to the Zig-Zag sequence order (for the second variant). As a result, we receive a representation C_w of a marked image.
3. Return to the spatial domain by calculating a two-dimensional IFPT. This step can be also implemented in a row-column approach by applying the IFPT to the rows (columns) and then to the columns (rows) of the C_w representation. This corresponds to the following operation in a matrix form: $X_w = U^T C_w U$.

The watermark extraction procedure takes at its input an image with an embedded watermark, which may have been subject to possible attacks. Such an image is designated as $\overline{X}_w$. The extraction procedure is then dependent on the adopted implementation variant of the method (see Fig. 6 and 7).

Procedure II (Watermark extraction).

1. Transform an input image with the embedded watermark $\overline{X}_w$ into the domain of a two-dimensional FPT by using the row-column approach. We can write then: $\overline{C}_w = U\overline{X}_w U^T$.
2. Depending on the adopted implementation variant of the method, we extract the watermark according to the equation (7) (for the first variant), or the watermark will take the form of the M number of FPT coefficients selected in accordance with the adopted Zig-Zag sequence order (for the second variat). The result of this operation is an extracted watermark r eferred to as w^*.

The form of a fast parametric transform is selected automatically in relation to the criterion of maximizing the separability measure s for a given input image X_0 (with size N on N pixels, where N is an integer power of two) and a predetermined type of attack. For this purpose, the classic genetic algorithm was used. Taking into account the linear separability of the two-dimensional FPT (see Proc. I and II), it is clear that only the one-dimensional FPT with the number N points will be adapted. Then, in accordance with the considerations from Section 4, the role of a single chromosome is to represent in the form of a set of L-bit integers $\{b_{ij}\}$ for $i = 0, 1, \ldots, \log_2 N - 1$ and $j = 0, 1, \ldots, N/2 - 1$ the values of FPT parameters, i.e. parameters α_{ij}, (see formula (5)), which in combination with the assumed fast structure (see Fig. 2) allow to determine the form of FPT, including the matrix representation U. Let P be the population size. In this case, we have P chromosomes, i.e. P sets of parameters $\{b_{ij}^p\}$ for $p = 0, 1, \ldots, P - 1$, which describe a P number of various U_p forms of FPT. In addition, $\{w_k\}$ for $k = 0, 1, \ldots, K - 1$ denotes a set of M-element watermarks, wherein these elements are the realizations of a random variable with a normal distribution of zero expected value and variance 1, i.e. $w_k(i) \in \mathcal{N}(0, 1)$ for $i = 0, 1, \ldots, M - 1$. In the case of the classical genetic algorithm there should be also determined the

number of epochs T, as well as the crossover ε_C and mutation ε_M probabilities. The value of coefficient η, which determines the strength of watermarking, should be also determined. The procedure for adaptive selection of the form of FPT is formulated below.

Procedure III (Adaptive selection of the form of a fast parametric transform).

1. Assign initial values in the form of integers taken with an equal probability from the set: $\{0,1,\ldots,2^L-1\}$ to the parameters $\{b_{ij}^p\}$ for $p=0,1,\ldots,P-1$, $i=0,1,\ldots,\log_2 N-1$ and $j=0,1,\ldots,N/2-1$,
2. Iterating over $p=0,1,\ldots,P-1$, i.e. over all sets of parameters, find subsequent forms of FPTs by mapping the values of b_{ij}^p parameters to the values of rotation angles according to formula (5).
3. Having the given form of FPT, perform the following actions by iterating over all watermarks from the set $\{w_k\}$ for $k=0,1,\ldots,K-1$, i.e.: embed the watermark (see Proc. I), conduct the given attack, extract the watermark (see Proc. II). The result is a set of extracted watermarks, designated as $\{w_k^*\}$.
4. For the given FPT and the set of extracted watermarks $\{w_k^*\}$, determine the measure of separability s_p according to formula (1). The value of this measure becomes simultaneously the value of the fitting function for the given chromosome (a set of parameters).
5. Keep the form, i.e. the values of parameters $\{b_{ij}^p\}$, for the best adapted chromosome (the maximum among s_p values).
6. Based on the set of values $\{s_p\}$ for $p=0,1,\ldots,P-1$, select chromosomes forming a new population for the next epoch using known approaches, e.g. the roulette method or tournament selection (see [33]).
7. With regard to the chromosomes emerged in the selection process, i.e. a new population, use genetic cross-over and mutation operators in accordance with the given probabilities ε_C and ε_M.
8. Repeat the steps listed in items 2–7 for each epoch, i.e. T times.

As a result of the use of Procedure III, we obtain the form of FPT (i.e. values of parameters b_{ij}, and hence also values of angles of rotation α_{ij}), which reached the highest value of the separability measure during the number of T epochs of the genetic algorithm.

6. Experimental research

The subject of the conducted research was an experimental verification of the effectiveness of fast parametric transforms in the tasks of watermarking of digital images. For this purpose, a number of practical tests were carried out based on sample images belonging to two classes, i.e. natural images (see Fig. 5 (a)), as well as images constituting an example of engineering technical documentation, i.e. diagrams from Fig. 5b. The images considered here are 8-bit grayscale with size of 256 by 256 pixels. Representative results in the form of the value of the separability measure determined for DCT (s_{DCT}) and FPT (s_{FPT}), as well as their differences ($s_{\mathrm{FPT}}-s_{\mathrm{DCT}}$), for various types of attacks and strengths of watermarks embedding, are presented in Tables 1-4 as mean values averaged over four images from each of the classes. It should be noted that the DCT is by default used in the Cox et al. and Barni et al. methods. Additionally, to facilitate interpretation of the obtained results, the percentage index $\chi_{\%}$ (see formula (8)) of improvement of separability was introduced, which is defined as the percentage ratio of the actual improvement in separability resulting from the use of FPT, i.e. the difference $(s_{\mathrm{DCT}}-s_{\mathrm{FPT}})$, to the theoretically possible improvement value calculated as a difference $(1-s_{\mathrm{DCT}})$. Thus, we have:

$$\chi_{\%}=\left(\frac{s_{\mathrm{FPT}}-s_{\mathrm{DCT}}}{1-s_{\mathrm{DCT}}}\right)\cdot 100\ \ [\%], \tag{8}$$

where s_{DCT} and s_{FPT} describe the separability values obtained with DCT and FPT respectively.

6.1. Research methodology. The process of watermarking of images was implemented in two variants, according to the Spread Spectrum approach (see Section 2). The first variant was the implementation of the Cox et al. method (see [3]), while the second one was based on the Barni et al. method proposed in [4]. In both cases, the watermarking process was carried out in the domain of fast parameteric transform (see Section 4). The form of the transformation, described by a set of parameters, was automatically selected in the process of evolutionary adaptation for the given pair: an input image – a possible attack. By assuming linear separability of the two-dimensional FPT, only the one-dimensional transform with the number of N points was subject to adaptation (assuming square images with a resolution of N on N pixels). The manner in which watermarks are embedded and extracted was specified within Procedures I and II. Between embedding and extraction stages there is a probability of attack, i.e. an intentional or accidental introduction of distortions to the marked image X_w, which can significantly affect an accuracy or even completely prevent the detection of whether a given image has been watermarked or whether it is not true (see Fig. 6 and 7). The following types of attacks were considered in the research:

Saving to bitmap. Under this name there is an operation of saving the marked image X_w to a BMP file. For this purpose, quantization of pixel values to integers within the range $\{0,1,\ldots,255\}$ is required. The introduced distortion to the image would be the quantization noise.

Noise filtration. This operation was implemented as a classical two-dimensional convolutional filtration scheme calculated for the X_w image and a mask with a dimension of 3 on 3 elements and the coefficients: $(1/9)[1,1,1,1,1,1,1,1,1]$.

Sharpening filtration. For this purpose the two-dimensional convolution filtration, was also used, with a rectangular mask of size 3 on 3 elements, which was filled with the following coefficients: $(1/4)[0,-2,0,-2,12,-2,0,-2,0]$.

Median filtration. This popular image filtration method consists in moving a square window with a dimension of 3 by 3 elements over the X_w image, with the result of filtration being the median of the pixel values of the image lying under the window in each step (see [40]).

Saving to JPEG file. It consists in saving the X_w image to a file in accordance with the JPEG standard with a quality factor of $q = 15$. The distortions introduced here are the sum of the quantization noise and the low-pass filtering.

Posterization. In other words this is a reduction of the number of shades of gray from 256 possible values here to the assumed number of 16 resulting values. The reduction in the number of shades was accomplished by using uniform quantization.

Contrast enhancement. Behind this term stands an elementary operation of linear stretching of the variation range of shades of pixels in the image to the entire possible set of values, i.e.: $\{0, 1, \ldots, 255\}$.

Histogram equalization. For this purpose, the basic algorithm of histogram equalization based on cumulative histogram, i.e. $H_C(m)$ for $m = 0, 1, \ldots, 255$, was used (see [40]). Then, if we assume that $0 \leq x \leq 255$ is the pixel value taken from an input image X_w, then the value saved to the resulting image $\overline{X}_w$ would take the following form: $\bar{x} = 255 \cdot H_C(x)$.

As already mentioned, the form of one-dimensional FPT with the number $N = 256$ points is automatically selected based on the evolutionary algorithm. For this purpose, the classical genetic algorithm was used in this study (see Section 4). Then, the role of a single chromosome is to represent the FPT form in a set of L-bit coefficients, which are integers, and which are respectively mapped to the angles of rotation for FPT base operations (see Section 4). During the experiments, the number $L = 8$ bits per one rotation angle for the base operation was assumed. The following values were assigned to the remaining parameters determining the behavior of the genetic algorithm: number of epochs $T = 200$, population size $P = 20$, crossover probabilities and mutations at $\varepsilon_C = 0.8$ and $\varepsilon_M = 0.2$, respectively. The fitness value of a single individual (see Section 4) was calculated on the basis of the separability measure (see Section 2), whose value was in turn determined on the set $K = 100$ watermarks, each with the length $M = 100$ elements. The process of adaptation of FPT itself was carried out according to Procedure III. When embedding watermarks using the Cox et al. approach, elements of watermarks were embedded in spectral coefficients by omitting the coefficient with the highest absolute value, while in the case of the Barni et al. method the first element resulting from the Zig-Zag sequence order was omitted. It should be noted that the maximization of the separability measure s guarantees an increase in the distance measured between the correlation of the watermark and its extracted form, and the correlation calculated between the same watermark and the extracted forms of other randomly selected watermarks. In the case of the Cox et al. [3] and Barni et al. [4] methods, the final output of the watermarking system takes the binary form, i.e. it allows to answer "yes" or "no" to the question whether the given X_w image has been marked using the watermark of the known form w? The final decision is then made based on the given threshold and the correlation value (see Section 2) calculated between the known watermark w and the extracted watermark w^*. Thus, the choice of the optimization criterion, which consists here in maximization of the separability measure, seems to be fully justified. In the research process, the elements of watermarks were taken as realizations of a random variable with normal distribution (see Section 5).

6.2. Results of experimental research. Based on the analysis of results[1] in Tables 1–4 it can be clearly observed that the use of the FPT allowed to obtain results that were much better than the results of the DCT, except for few cases for small values of the η coefficient (understood in the sense of the considered variant of the method) where both transforms gave identical results. In the first implementation variant of the method, which was based on the Cox et al. approach, the highest increase in separability for natural images was observed for the attacks: "Sharpening filtration", "Median filtration", "Posterization", "Contrast enhancement", "Histogram equalization". Here, the value of the $\chi_{\%}$ coefficient remained close to 30%, often yielding results equal to and above 50%. It should also be noted that the improvement of separability achieved with the FPT has been observed to a large extent already for small values of the η coefficient, i.e. for $\eta \geq 5$, which in turn indicates a high sensitivity of the transformation and good adaptation to the characteristics of the images. The lowest values of the $\chi_{\%}$ coefficient were obtained for attacks characterized as low-pass filtration, i.e. for "Noise filtration" and "Saving to JPEG ($q = 15$)". This can be explained by the high separability values obtained using the DCT, so that the possible margin of improvement of these values was much smaller. For the second class of considered images, i.e. for technical diagrams, similar results were observed (see Table 3). Only in the case of "Histogram equalization" attack we could observe an increase of separability at a high level, i.e. above 30%, already for the coefficient $\eta \geq 1$.

The results obtained for the implementation variant of the method based on the Barni et al. approach showed very poor properties of DCT. For both image classes, all the attacks under consideration and the considered values of the η coefficient, the DCT did not allow for separation of watermarks, which resulted in a zero values of separability measure. It should be noted that the level of watermark separation obtained by using the FPT was high almost in all cases, i.e. excluding the "Noise filtering", "Median filtering" and "Saving to JPEG file ($q = 15$)" attacks for natural images, as well as "Noise filtering" and "Saving to JPEG ($q = 15$)" for technical diagrams, and depending on the strength of embedding the watermark,

[1]It should be noted that in Tables 2 and 3 we do not present results in the form of s_{DCT} and $s_{\text{FPT}} - s_{\text{DCT}}$ values due to the fact that in the case of Barni et al. approach the DCT did not allow to obtain the values of separation measure higher than zero (i.e. $s_{\text{DCT}} = 0$) for both classes of images, all of the considered types of attacks and all values of η coefficient.

Table 1
The experimental results obtained for natural images and the first implementation variant (see paper [3])

	$\eta = 1$	$\eta = 5$	$\eta = 8$	$\eta = 10$	$\eta = 15$	$\eta = 20$	$\eta = 25$	$\eta = 30$
Saving to bitmap								
s_{DCT}	0.823482	0.823545	0.831296	0.837954	0.852758	0.861988	0.860340	0.861606
s_{FPT}	0.865169	0.865334	0.870563	0.874409	0.868487	0.867152	0.865868	0.866252
$s_{FPT} - s_{DCT}$	0.041686	0.041789	0.039267	0.036455	0.015730	0.005165	0.005528	0.004646
$\chi_{\%}[\%]$	24	24	23	22	11	4	4	3
Noise filtration								
s_{DCT}	0.000000	0.317979	0.524432	0.603623	0.713971	0.765747	0.795330	0.813763
s_{FPT}	0.054438	0.463081	0.642659	0.709394	0.784720	0.816824	0.831942	0.840082
$s_{FPT} - s_{DCT}$	0.054438	0.145102	0.118227	0.105771	0.070750	0.051078	0.036612	0.026320
$\chi_{\%}[\%]$	5	21	24	26	24	21	17	14
Sharpening filtration								
s_{DCT}	0.092786	0.141193	0.315498	0.415338	0.577951	0.668724	0.723273	0.757196
s_{FPT}	0.213462	0.454946	0.639013	0.705967	0.784626	0.807031	0.816846	0.821533
$s_{FPT} - s_{DCT}$	0.120676	0.313753	0.323515	0.290629	0.206675	0.138306	0.093573	0.064337
$\chi_{\%}[\%]$	13	37	48	50	49	41	33	26
Median filtration								
s_{DCT}	0.252764	0.252822	0.263777	0.288696	0.424027	0.532591	0.608687	0.663656
s_{FPT}	0.447451	0.447814	0.461426	0.495656	0.600665	0.687432	0.735724	0.764488
$s_{FPT} - s_{DCT}$	0.194687	0.194992	0.197650	0.206961	0.176638	0.154841	0.127037	0.100833
$\chi_{\%}[\%]$	26	26	27	29	31	33	33	30
Saving to JPEG file (quality factor $q = 15$)								
s_{DCT}	0.010529	0.672448	0.767643	0.795664	0.821256	0.845133	0.845524	0.850062
s_{FPT}	0.121141	0.718828	0.802110	0.847829	0.847957	0.855306	0.856647	0.855923
$s_{FPT} - s_{DCT}$	0.110612	0.046380	0.034467	0.052165	0.026701	0.010173	0.011123	0.005860
$\chi_{\%}[\%]$	11	14	15	25	15	7	8	7
Posterization								
s_{DCT}	0.393284	0.393639	0.406109	0.430686	0.548339	0.630023	0.690199	0.736112
s_{FPT}	0.593053	0.593114	0.603093	0.635313	0.698317	0.750348	0.780186	0.803757
$s_{FPT} - s_{DCT}$	0.199768	0.199476	0.196984	0.204627	0.149978	0.120324	0.089988	0.067645
$\chi_{\%}[\%]$	32	31	32	35	32	30	27	24
Contrast enhancement								
s_{DCT}	0.000000	0.000000	0.000000	0.000000	0.003846	0.031711	0.056753	0.094982
s_{FPT}	0.000273	0.186910	0.281635	0.331165	0.424498	0.498533	0.556462	0.603230
$s_{FPT} - s_{DCT}$	0.000273	0.186910	0.281635	0.331165	0.420652	0.466822	0.499709	0.508249
$\chi_{\%}[\%]$	0	19	28	33	42	49	54	57
Histogram equalization								
s_{DCT}	0.000000	0.000000	0.000000	0.000000	0.000000	0.000000	0.000000	0.000000
s_{FPT}	0.116769	0.117109	0.131131	0.159793	0.260550	0.360312	0.436956	0.501315
$s_{FPT} - s_{DCT}$	0.116769	0.117109	0.131131	0.159793	0.260550	0.360312	0.436956	0.501315
$\chi_{\%}[\%]$	12	12	13	16	26	36	44	50

Table 2
The experimental results obtained for natural images and the second implementation variant (see paper [4])

	$\eta = 10$	$\eta = 12$	$\eta = 15$	$\eta = 20$	$\eta = 30$	$\eta = 40$	$\eta = 50$	$\eta = 55$
Saving to bitmap								
s_{FPT}	0.574476	0.615008	0.670988	0.746675	0.821282	0.844186	0.852932	0.856138
$\chi_{\%}[\%]$	57	62	67	75	82	84	85	86
Noise filtration								
s_{FPT}	0.000000	0.001858	0.023853	0.068741	0.154801	0.231743	0.293327	0.321199
$\chi_{\%}[\%]$	0	0	2	7	15	23	29	32
Sharpening filtration								
s_{FPT}	0.628280	0.685599	0.743705	0.797904	0.841416	0.851053	0.854665	0.855836
$\chi_{\%}[\%]$	63	69	74	80	84	85	85	86
Median filtration								
s_{FPT}	0.031874	0.049273	0.091063	0.171546	0.297557	0.402386	0.470172	0.497326
$\chi_{\%}[\%]$	3	5	9	17	30	40	47	50
Saving to JPEG file (quality factor $q = 15$)								
s_{FPT}	0.000000	0.011712	0.058537	0.159214	0.328917	0.457380	0.546104	0.580268
$\chi_{\%}[\%]$	0	1	6	16	33	46	55	58
Posterization								
s_{FPT}	0.540375	0.584841	0.645000	0.720821	0.808560	0.824346	0.837877	0.841489
$\chi_{\%}[\%]$	54	58	65	72	81	82	84	84
Contrast enhancement								
s_{FPT}	0.514244	0.592184	0.671766	0.751797	0.819360	0.842443	0.851962	0.855539
$\chi_{\%}[\%]$	51	59	67	75	82	84	85	86
Histogram equalization								
s_{FPT}	0.587036	0.627129	0.683626	0.753898	0.824316	0.843334	0.851654	0.854888
$\chi_{\%}[\%]$	59	63	68	75	82	84	85	85

it varied within the range of $0 < s_{\mathrm{FPT}} < 0.58$ for natural images and within $0 < s_{\mathrm{FPT}} < 0.44$ for technical diagrams. With respect to the $\chi_{\%}$ coefficient, it allowed to obtain results even at the level above 70%, which can be observed for attacks: "Save to BMP file", "Sharpening filtration", "Posterization", "Contrast enhancement" and "Histogram equalization" for the coefficient value $\eta \geq 30$. In the case of technical diagrams, "Median filtration" was not considered because, due to the characteristics of the images, this attack introduced too high distortion.

In the case of the Cox et al. approach [3] and the considered values of η coefficient, which determines the strength of embedment of watermarks, and $\eta \in \{1,5,8,10,15,20,25,30\}$, the *PSNR* quality measure of images reached the following values: 76, 62, 59, 56, 52, 50, 48, 46 dB for both classes of images, while the *SSIM* index value varied from 0.993 to 1.000. In turn, for the implementation of Barni et al. approach [4], where the embedding strength had to be proportionally higher and took values: $\eta \in \{10,12,15,20,30,40,50,55\}$, respectively, the process of watermarking generated distortions that allowed to obtain image quality measured with the *PSNR* measure at the following levels: 56, 54, 52, 50, 46, 44, 42,41 dB. Here, the value of the SSIM index was close to 1.000. Thus, in the light of the adopted measures, the quality of images after watermarking in all the considered cases can be considered to be sufficiently high.

7. Summary and conclusions

This paper proposes a new method for watermarking digital images based on known spread spectrum approaches, namely the Cox et al. approach [3] and the Barni et al. approach [4]. Here, however, unlike the aforementioned approaches, watermarking of images does not take place in the domain of discrete cosine transform (DCT), but in an automatically selected domain of

Table 3
The experimental results obtained for technical diagrams and the first implementation variant (see paper [3])

	$\eta = 1$	$\eta = 5$	$\eta = 8$	$\eta = 10$	$\eta = 15$	$\eta = 20$	$\eta = 25$	$\eta = 30$
Saving to bitmap								
s_{DCT}	0.845450	0.845337	0.846561	0.849439	0.855820	0.858820	0.858405	0.859518
s_{FPT}	0.866459	0.866654	0.869293	0.871147	0.863931	0.864014	0.862742	0.864948
$s_{FPT} - s_{DCT}$	0.021009	0.021318	0.022732	0.021708	0.008111	0.005194	0.004338	0.005430
$\chi_{\%}[\%]$	13	14	15	14	6	4	3	4
Noise filtration								
s_{DCT}	0.000000	0.083461	0.133834	0.165056	0.239372	0.311790	0.364540	0.414213
s_{FPT}	0.006858	0.202437	0.329027	0.392804	0.500613	0.572844	0.624133	0.660834
$s_{FPT} - s_{DCT}$	0.006858	0.118976	0.195194	0.227749	0.261242	0.261055	0.259593	0.246621
$\chi_{\%}[\%]$	1	14	23	28	32	33	35	35
Sharpening filtration								
s_{DCT}	0.000000	0.000000	0.000000	0.000000	0.018486	0.069619	0.125797	0.176762
s_{FPT}	0.008695	0.211706	0.369042	0.447895	0.579159	0.650575	0.692779	0.720773
$s_{FPT} - s_{DCT}$	0.008695	0.211706	0.369042	0.447895	0.560674	0.580956	0.566982	0.544011
$\chi_{\%}[\%]$	1	21	37	45	57	63	65	66
Median filtration								
s_{DCT}	—	—	—	—	—	—	—	—
s_{FPT}	—	—	—	—	—	—	—	—
$s_{FPT} - s_{DCT}$	—	—	—	—	—	—	—	—
$\chi_{\%}[\%]$	—	—	—	—	—	—	—	—
Saving to JPEG file (quality factor $q = 15$)								
s_{DCT}	0.000000	0.380462	0.561502	0.644780	0.739069	0.772305	0.797457	0.816403
s_{FPT}	0.002210	0.554787	0.717421	0.774610	0.814145	0.834812	0.841898	0.852852
$s_{FPT} - s_{DCT}$	0.002210	0.174326	0.155919	0.129830	0.075075	0.062507	0.044441	0.036449
$\chi_{\%}[\%]$	0	25	33	36	28	27	21	19
Posterization								
s_{DCT}	0.047282	0.047149	0.051189	0.074093	0.149538	0.275925	0.405348	0.526201
s_{FPT}	0.220473	0.221270	0.239767	0.264227	0.361752	0.489589	0.561748	0.641334
$s_{FPT} - s_{DCT}$	0.173191	0.174122	0.188578	0.190133	0.212214	0.213664	0.156400	0.115133
$\chi_{\%}[\%]$	19	19	21	22	27	31	29	26
Contrast enhancement								
s_{DCT}	0.000000	0.120285	0.458779	0.541428	0.685840	0.757434	0.791574	0.812732
s_{FPT}	0.000000	0.480386	0.730147	0.791918	0.820512	0.836547	0.846257	0.847796
$s_{FPT} - s_{DCT}$	0.000000	0.360102	0.271368	0.250491	0.134672	0.079113	0.054683	0.035064
$\chi_{\%}[\%]$	0	41	47	52	38	30	25	18
Histogram equalization								
s_{DCT}	0.123206	0.123417	0.130065	0.145258	0.237268	0.323370	0.397543	0.458532
s_{FPT}	0.452656	0.453015	0.467605	0.492142	0.574294	0.647843	0.697044	0.732984
$s_{FPT} - s_{DCT}$	0.329450	0.329598	0.337540	0.346884	0.337027	0.324473	0.299501	0.274453
$\chi_{\%}[\%]$	39	39	41	42	46	50	51	51

Table 4
The experimental results obtained for technical diagrams and the second implementation variant (see paper [4])

	$\eta = 10$	$\eta = 12$	$\eta = 15$	$\eta = 20$	$\eta = 30$	$\eta = 40$	$\eta = 50$	$\eta = 55$
Saving to bitmap								
s_{FPT}	0.414060	0.465774	0.539711	0.644125	0.750628	0.795122	0.817771	0.825066
$\chi_{\%}[\%]$	41	47	54	64	75	80	82	83
Noise filtration								
s_{FPT}	0.000000	0.000000	0.000000	0.017398	0.094176	0.184665	0.256579	0.288003
$\chi_{\%}[\%]$	0	0	0	2	9	18	26	29
Sharpening filtration								
s_{FPT}	0.467320	0.537654	0.615157	0.699326	0.781708	0.811898	0.825432	0.829699
$\chi_{\%}[\%]$	47	54	62	70	78	81	83	83
Median filtration								
s_{FPT}	—	—	—	—	—	—	—	—
$\chi_{\%}[\%]$	—	—	—	—	—	—	—	—
Saving to JPEG file (quality factor $q = 15$)								
s_{FPT}	0.006398	0.019140	0.047547	0.113705	0.223529	0.325802	0.404595	0.443349
$\chi_{\%}[\%]$	1	2	5	11	22	33	40	44
Posterization								
s_{FPT}	0.193528	0.244946	0.347062	0.497187	0.699689	0.773306	0.806829	0.818570
$\chi_{\%}[\%]$	19	24	35	50	70	77	81	82
Contrast enhancement								
s_{FPT}	0.364917	0.441340	0.556710	0.667971	0.768244	0.808167	0.827725	0.833559
$\chi_{\%}[\%]$	36	44	56	67	77	81	83	83
Histogram equalization								
s_{FPT}	0.850405	0.855597	0.863018	0.869579	0.875738	0.874997	0.874599	0.874397
$\chi_{\%}[\%]$	85	86	86	87	88	87	87	87

fast parameteric transformation (FPT). The undeniable advantage of the FPT over transformations with fixed base vectors, including DCT, is the ability to adapt their forms to the specific requirements of the tasks performed while maintaining fast computational structures. In the proposed method, the form of the transform was subject to adaptation to the given pair: watermarked image – type of attack, assuming a class of watermarks with elements taken as realizations of a random variable with normal distribution. The experiment carried out in this way allowed to obtain the best possible results in the sense of adapting the transform to the needs of the task being performed. An analysis of obtained results allowed to conclude unambiguously that the use of FPT in the tasks of watermarking of digital images is justified and may result in a significant improvement of the effectiveness of this technique. The improvement of watermarking effectiveness, which is expressed in this paper in the form of the watermark separability measure, may amount to over 80% of the value of the decrease in the efficiency of the DCT calculated against the theoretically largest possible value of separability. Often, however, an improvement of over 20% was achieved. It should be emphasized here that the parametrization used in the paper did not use the number of all possible parameters, which resulted from two facts: (a) only part of the used structure (little above half of all base operations) was parametrized, (b) image transformation into the FPT domain was implemented using one-dimensional transform and the row-column approach. In conclusion, by taking into account high computational efficiency of fast parametric transforms and results obtained in image watermarking, which are better than those obtained with commonly used DCT, it can be clearly stated that FPTs can be successfully applied to the tasks of watermarking of digital images, including various classes of images, i.e. both natural as well as technical diagrams. The possibility of adaptation of the embedment domain can be particularly important in the light of new challenges posed to watermarking algorithms, e.g. such as the watermarking of stereoscopic images (see [41, 42]).

References

[1] P. Lipiński, *Robust watermarks in images. Adaptive selection of embedment domain* (in Polish), EXIT, Warsaw, 2013.

[2] B. Furht, E. Muharemagic, and D. Socek, *Multimedia Encryption and Watermarking*, Springer, 2005.

[3] I.J. Cox, J. Kilian, F.T. Leighton, and T. Shamoon, "Secure spread spectrum watermarking for multimedia", *IEEE Transactions on Image Processing* 6 (12), 1673–1687 (1997).

[4] M. Barni, F. Bartolini, V. Cappellini, and A. Piva, "A DCT-domain system for robust image watermarking", *Signal Processing* 66 (3), 357–372 (1998).

[5] K.R. Rao and P. Yip, *Discrete Cosine Transform. Algorithms, Advantages, Applications*, Academic Press, 1990.

[6] D. Puchala, "Approximating the KLT by Maximizing the Sum of Fourth-Order Moments", *Signal Processing Letters IEEE* 20 (3), 193–196 (2013).

[7] D. Puchala, *Fast linear parametric transforms. Computational structures and adaptation techniques* (in Polish), Exit, Warsaw, 2017.

[8] B. Chen and G.W. Wornell, "Quantization index modulation: a class of provably good methods for digital watermarking and information embedding", *IEEE Trans. on Information Theory* 47 (4), 1423–1443 (2001).

[9] S. Craver, N. Memon, B.-L. Yeo, and M.M. Yeung, "Resolving rightful ownerships with invisible watermarking techniques: limitations, attacks, and implications", *IEEE Journal on Selected Areas in Communications* 16 (4), 573–586 (1998).

[10] N.F. Johnson and S. Jajopdia, "Steganalysis of images created using current steganography software", *Proc. of the Second International Workshop on Information Hiding* 1525, 273–289 (1998).

[11] E. Koch, J. Rindfrey, and J. Zhao, "Copyright protection of multimedia data", *Proc. of the International Conference on Digital Media and Electronic Publishing*, 1994.

[12] Ch.-H. Lee, H.-S. Oh, Y. Baek, and J.-K. Lee, "Adaptive digital image watermarking using variable size of blocks in frequency domain", *Proc. IEEE Region 10 Conference TENCON99* 1, 702–705 (1999).

[13] Z. Wei, H. Li, J. Dai, and S. Wang, "Image watermarking based on genetic algorithm", *Proc. of IEEE International Conference On Multimedia and Expo*, 1117–1120 (2006).

[14] R. Dugad, K. Ratakonda, and N. Ahuja, "A new wavelet-based scheme for watermarking images", *Proc. International Conference On Image Processing ICIP* 2, 419–423 (1998).

[15] S. Tsekeridou and I. Pitas, "Embedding self-similar watermarks in the wavelet domain", *Proc. IEEE International Conference On Acoustics, Speech, and Signal Processing ICASSP* 6, 1967–1970 (2000).

[16] M. Barni, F. Bartolini, V. Cappelilini, A. Lippi, and A. Piva, "A dwt-based technique for spatio-frequency masking of digital signatures", *Proc. of SPIE Conference* 3657 (1999).

[17] D. Puchala, K. Stokfiszewski, B. Szczepaniak, and M. Yatsymirskyy, "Effectiveness of Fast Fourier Transform Implementations on GPU and CPU", *Electrical Review (Przegląd Elektrotechniczny)*, R.92 (7), 69–71 (2016).

[18] D. Barina, M. Kula, M. Matysek, and P. Zemcik, "Accelerating discrete wavelet transforms on GPUs", *ICIP 2017, IEEE International Conference on Image Processing*, 2707–2710 (2017).

[19] M. Półrola and A. Wojciechowski, "Real-Time Hand Pose Estimation Using Classifiers", *Computer Vision and Graphics, ICCVG 2012, Springer Lecture Notes in Computer Science* 7594, 573–580 (2012).

[20] A. Wasiljew and K. Murawski, "A new CUDA-based GPU implementation of the two-dimensional Athena code", *Bull. Pol. Ac.: Tech.* 61 (1), 239–250 (2013).

[21] M. Wawrzonowski, M. Daszuta, D. Szajerman, and P. Napieralski, "Mobile devices' GPUs in cloth dynamics simulation", FedCSIS 2017, *Proc. of the 2017 Federated Conference on Computer Science and Information Systems*, 1283–1290 (2017).

[22] K. Stokfiszewski, D. Puchala, and M. Yatsymirskyy, "Effectiveness of GPU Realizations of Parallel Prefix-Sums Computation Algorithms", *CSIT 2018, XIII-th International Scientific and Technical Conference Computer Science and Information Technologies*, 436–439 (2018).

[23] K. Deb, M.S. Al-Seraj, M.M. Hoque and M.I.H. Sarkar, "Combined DWT-DCT based digital image watermarking technique for copyright protection", *7th International Conference on Electrical and Computer Engineering, Dhaka*, 458–461 (2012).

[24] A. Akter, Nur-E-Tajnina and M.A. Ullah, "Digital image watermarking based on DWT-DCT: Evaluate for a new embedding algorithm", *International Conference on Informatics, Electronics & Vision (ICIEV), Dhaka*, 1–6 (2014).

[25] L. Xie and G.R. Arce, "Joint wavelet compression amd authentication watermarking", *Proc. International Conference On Image Processing ICIP* 2, 427–431 (1998).

[26] Ch.-J.H. Chu and A.W. Wiltz, "Luminance channel modulated watermarking of digital images", *Proc. of SPIE Wavelet Applications Conference*, 1999.

[27] X. Li, X. Xue, "A novel blind watermarking based on lattice vector quantization", *Proc. Canadian Conference on Electrical and Computer Engineering* 3, 1823–1826 (2004).

[28] I.J. Cox, *Digital Watermarking and Steganography*, Morgan Kaufman, 2008.

[29] N. Ahmed and K.R. Rao, *Orthogonal Transforms for Digital Signal Processing*, Springer-Verlag, 1975.

[30] S. Bouguezel, O. Ahmad, and M.N.S. Swamy, "A New Class of Reciprocal-Orthogonal Parametric Transforms", *IEEE Transactions on Circuits and Systems-I: Regular Papers* 56 (4), 795–805 (2009).

[31] S. Agaian, K. Tourshan, and J.P. Noonan, "Parametric Slant–Hadamard Transforms With Applications", *IEEE Signal Processing Letters* 9 (11) (2002).

[32] M. Morháč and V. Matoušek, "An adaptive fast transform algorithm for multi-dimensional data compression", *Elsevier Signal Processing* 43, 29–37 (1995).

[33] S.N. Sivanandam and S.N. Deepa, *Introduction to Genetic Algorithms*, Springer, 2008.

[34] L. Rutkowski, *Computational Intelligence. Methods and Techniques*, Springer, 2008.

[35] B. Borowska, "Dynamic Inertia Weight in Particle Swarm Optimization", *Springer Advances in Intelligent Systems and Computing, CSIT 2017, XII International Scientific and Technical Conference Computer Science and Information Technologies* 689, 79–88 (2018).

[36] S. Opałka, B. Stasiak, D. Szajerman, and A. Wojciechowski, "Multi-Channel Convolutional Neural Networks Architecture

Feeding for Effective EEG Mental Tasks Classification", *Sensors* 18 (3451) (2018).

[37] P. Lipiński and J. Stolarek, "Digital watermarking enhancement using wavelet filter parametrization", *Adaptive And Natural Computing Alogrithms* 6593, 330–339 (2011).

[38] J. Stolarek and P. Lipiński, "Improving watermark resistance againts removal attacks using orthogonal wavelets adaptation", *Lecture Notes In Computer Science* 7147, 588–599 (2012).

[39] P. Lipiński, "Watermarking software in practical applications", *Bull. Pol. Ac.: Tech.* 59 (1), 21–25 (2011).

[40] R.C. Gonzalez and R.E. Woods, *Digital Image Processing*, Global Edition, Pearson Education Limited, 2017.

[41] A. Al-Haja, M.E. Farfourab, and A. Mohammad, "Transform-based watermarking of 3D depth-image-based-rendering images", *Measurement* 95, 405–417 (2017).

[42] K. Fornalczyk, P. Napieralski, and D. Szajerman, "Stereoscopic Image Perception Quality Factors", *22nd International Conference on Mixed Design of Integrated Circuits & Systems*, 129–133, 2015.

Appendix

The list of abbreviations used in the text of the paper:

BMP – stands for bitmap image file (popular raster graphics image file format),
DCT – Discrete Cosine Transform,
DWT – Discrete Wavelet Transform,
FMR – False Match Rate,
FNMR – False Non-Match Rate,
FPT – Fast Parametric Transform,
IFPT – Inverse Fast Parametric Transform,
JPEG – Joint Photographic Experts Group (popular standard for lossy compression of images),
MSE – Mean Square Error,
PSNR – Peak Signal to Noise Ratio,
QIM – Quantization Index Modulation,
SSIM – Structural Similarity Index.